Article

Toughness, Reinforcing Mechanism, and Durability of Hybrid Steel Fiber Reinforced Sulfoaluminate Cement Composites

Kai Cui [1], Jun Chang [1,*], Mohanad Muayad Sabri Sabri [2] and Jiandong Huang [3,*]

1   School of Civil Engineering, Dalian University of Technology, Dalian 116024, China
2   Peter the Great St. Petersburg Polytechnic University, 195251 St. Petersburg, Russia
3   School of Civil Engineering, Guangzhou University, Guangzhou 510006, China
*   Correspondence: mlchang@dlut.edu.cn (J.C.); jiandong.huang@hotmail.com (J.H.)

Abstract: As a low-carbon ecological cement-based material, SAC (sulfoaluminate cement) has become a research hotspot. This study developed a SAC-based high-performance concrete material with good durability and high toughness. The mechanical properties of different scales of MSF (macro steel fiber) and mSF (micro steel fiber) reinforced sulfoaluminate cement-based composites were mainly studied, including their compressive strength, flexural strength, toughness index, and toughness ratio, and their resistance to sulfate erosion was characterized. The results show that adding MSF and HSF (hybrid steel fibers) can significantly improve concrete's compressive and flexural strength compared with the Plain group. The compressive strength of SSF1 (1% MSF) and SSF2 (1.5% MSF) increased by 10.9%, 19.6%, and the compressive strength of HSF1 (0.1% mSF, 1.4% MSF), HSF2 (0.2% mSF, 1.3%MSF), HSF3 (0.3% mSF, 1.2% MSF), and HSF4 (0.5% mSF, 1.0% MSF) increased by 23.9%, 33.7%, 37.0%, 29.3%, respectively, while the flexural strength of HSF1, HSF2, HSF3, and HSF4 groups increased by 51.4%, 84.9%, 88.1%, and 64.2%. Compared with the single steel fiber (SSF) group, the HSF group has higher initial crack strength, equivalent flexural strength, toughness index, and toughness ratio. Hybrid fibers have a higher synergistic effect when mSF content is 0.2–0.3% and MSF content is 1.2–1.3%. The mechanism of multi-scale reinforcement of hybrid-steel-fiber-enhanced sulfoaluminate cement-based composites was researched. MSF bridges macro-cracks, mSF bridges micro-cracks, and these two different scales of steel fibers, through filling, bridging, anchoring, pulling off, and pulling out, improve the toughness of composite materials. The mechanism of sulfate corrosion resistance of sulfoaluminate cement-based composites was obtained. SO_4^{2-} entered the matrix and reacted and formed AFt, filling the matrix's pores. The whole process is similar to the self-healing process of concrete.

Keywords: sulfoaluminate cement; toughness; reinforcing mechanism; resistance to sulfate erosion

1. Introduction

Concrete is widely used in the construction industry due to its low price and easy availability of raw materials [1]. The high brittleness and low tensile strain of ordinary concrete seriously restricts its development and cannot meet increasing engineering needs [2]. Along with the continuous development of the construction industry, higher requirements are being placed on cement and concrete materials [3–6]. On the one hand, cement and concrete materials are developing towards functionalization, intelligence, and high strength [7]. As a multi-phase material, the destruction of concrete is a complex process. The destruction of concrete starts from the appearance of microscopic cracks and gradually develops into macroscopic cracks, which eventually leads to the destruction of concrete. Therefore, there is a need to improve concrete properties and reduce and retard the development of concrete cracks. Improving crack resistance of concrete is usually accomplished via both micro-scale and macro-scale factors [8]. On the micro-scale, this is accomplished by adding micro–nano materials, such as carbon nanotubes (CNTs) [9–11], graphene nanoplates (GNPs) [12–15],

whiskers [16], or carbon fibers [17–20], and on the macro scale, by the addition of materials including steel fibers [21,22], PVA (polyvinyl alcohol fiber) fibers [23], and basalt fibers [24–26]. Usually, using a single fiber or material can only improve the performance of the concrete at its respective level. Therefore, it is necessary to use multi-scale, multi-type, and multi-performance materials to jointly enhance the toughness of concrete from both microscopic and macroscopic aspects.

Hybrid-fiber-reinforced concrete can prevent cracks at multiple scales and improve the mechanical properties of concrete and has been widely studied in recent years. Li et al. studied the flexural toughness of several different steel fiber and polypropylene fiber, tested the toughness test of 51 specimens, and concluded that the straight steel fiber and polypropylene fiber showed an obvious synergistic effect. The residual load deflection is significantly improved, the fullness of the curve is dramatically enhanced, and the bending toughness is improved significantly [27]. Huang et al. studied the seismic performance of steel fiber and polypropylene fibers. They found that the synergistic effect of hybrid fibers improved the ductility and energy dissipation capacity of fiber-reinforced concrete, and the axial compression improvement rate reached 15–20% [28]. Banthia et al. compared the flexural properties of two macroscopic steel fibers and plain concrete. They concluded that the hybrid fibers could effectively improve the performance of concrete, resulting in a significant synergistic effect [29]. Wu et al. studied the impact of different shapes of steel fibers on the bonding properties of UHPC; the flexural strength of corrugated steel fibers and hooked steel fibers increased by 8–28% and 17–50% [30]. Gao et al. studied the flexural toughness of steel-fiber-reinforced recycled concrete and found that when the content of steel fiber is less than 0.5%, the improvement of bending toughness is not apparent. When the content of steel fiber is 0.5–1%, the improvement effect of flexural toughness is obvious [31].

On the other hand, cement and concrete materials must be green, low-carbon, and environmentally friendly and reduce environmental pollution. Cement and concrete materials should develop in a sustainable fashion. In addition, China proposes to achieve a peak in carbon dioxide emissions by 2030 and to achieve carbon neutrality by 2060 [2]. The main ways to reduce carbon dioxide in the cement and concrete industry are to reduce and replace fossil fuels, such as using industrial by-product waste to prepare fuel, and reducing and replacing calcium carbonate raw materials, such as using steel slag and recycling aggregates, developing low-carbon cementitious materials, reducing energy consumption, researching and developing technologies such as carbon capture and utilization, and developing low-calcium clinker minerals, such as sulfoaluminate cement. SAC has high early strength, is fast-setting and -hardening, and has excellent durability. In addition, SAC is a low-carbon ecological cement, which is in line with the development of green building materials.

The above discussion shows that there are many types of research on hybrid-fiber-reinforced concrete at present, mainly on compressive strength, flexural toughness, and synergistic effects. The primary research material is OPC (ordinary Portland cement); there is a lack of research on the durability of hybrid-fiber-reinforced concrete, especially against sulfate attack. In addition, the research on the flexural toughness of low-carbon ecological SAC is exceptionally scarce, which severely limits the application of SAC. There is an urgent need to study the mechanical properties and flexural toughness and to explore the sulfate corrosion resistance of hybrid-fiber-reinforced sulfoaluminate cement-based materials.

This paper mainly studies the mechanical properties of hybrid-steel-fiber-reinforced sulfoaluminate cement-based materials, including compressive strength, flexural strength, and ratio of flexural strength to compressive strength. The toughness and sulfate-attack resistance of hybrid-steel-fiber-reinforced sulfoaluminate cement-based composites were investigated. The hybrid fibers' enhancement mechanism and sulfate-attack resistance mechanism on SAC-FRC were revealed.

2. Materials and Methods

2.1. Materials

Tangshan Polar Bear Co., Ltd. provided SAC. Elkem Materials Co., Ltd. provided SF (silica fume). Table 1 shows the chemical compositions of SAC and SF. A polycarboxylate superplasticizer (SP), produced by Chongqing Sansheng Building Material Co., Ltd., was used. The particle size of the sand was 0.12–0.83 mm, and two steel fibers, namely macro steel fibers (MSF) and micro steel fibers (mSF), were used. Figure 1 shows the morphologies of the two steel fibers.

Table 1. Chemical compositions of SAC and SF (wt%).

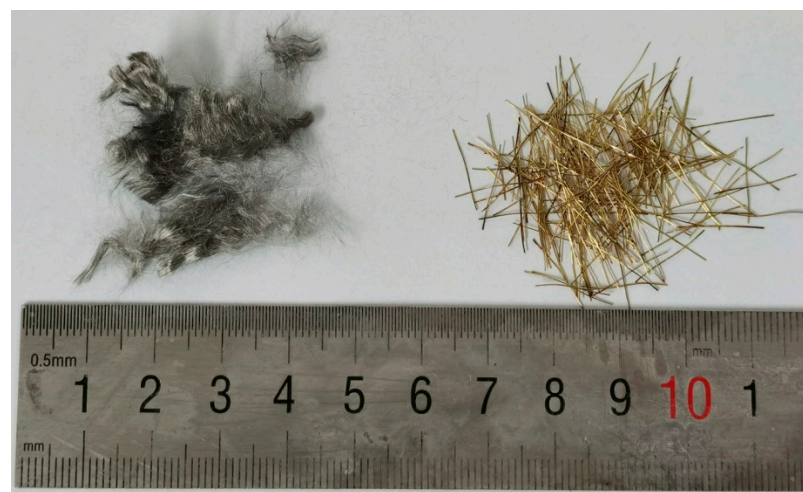| Type	Fe_2O_3	Al_2O_3	CaO	SO_3	MgO	SiO_2	TiO_2
SAC	2.15	16.34	46.08	12.45	2.52	19.15	1.31
SF	0.64	0.71	0.11	0.15	0.13	94.36	–

Figure 1. Morphologies of the two steel fibers.

2.2. Mix Proportions and Methods

The mix design is shown in Table 2. A sulfate corrosion resistance test of concrete was carried out according to the GB/T 50082-2009 and GB/T 749-2008 standards, and the full-immersion method was used. The evaluation indicators included the change in concrete strength, corrosion resistance coefficient evolution, and mass-loss rate.

Table 2. Mix design of mixtures.

Group	w/b	Cement	Silica Fume	Water	Sand	mSF (%)	MSF (%)	SP
Plain	0.34	1	0.15	0.391	1.1	0	0	2%
SSF-1	0.34	1	0.15	0.391	1.1	0	1%	2%
SSF-2	0.34	1	0.15	0.391	1.1	0	1.5%	2%
HSF-1	0.34	1	0.15	0.391	1.1	0.1%	1.4%	2%
HSF-2	0.34	1	0.15	0.391	1.1	0.2%	1.3%	2%
HSF-3	0.34	1	0.15	0.391	1.1	0.3%	1.2%	2%
HSF-4	0.34	1	0.15	0.391	1.1	0.5%	1.0%	2%

For the sulfate corrosion resistance test, a $4 \times 4 \times 16$ cm^3 test block was used, the formed specimen was placed in a standard curing room for curing for 28 days, and then the sulfate corrosion resistance test was started. The initial weight was measured, the test piece of the erosion group was placed into a prepared 5% Na_2SO_4 solution, the test piece of the Plain (control) group was placed into a clear water solution, the solution was changed every 30 days, and quality tests were conducted every 7 days for the erosion group and strength tests after curing for 28 days, 60 days, 90 days, 120 days, 150 days, and 180 days.

3. Results and Analysis

3.1. Compressive Strength

Figure 2 shows the compressive strength of FRC after curing for 28 days. FRC's compressive and flexural strengths can be improved to different degrees by adding a single MSF group and a hybrid fiber group (mSF, MSF). The compressive strengths of SSF1 and SSF2 increased by 10.9% and 19.6%, and the compressive strengths of HSF1, HSF2, HSF3, HSF4 increased by 23.9%, 33.7%, 37.0%, 29.3%, respectively. The increase in the compressive strength of the HSF (hybrid fiber group) was greater than that of the Plain group and the SSF (single fiber group). Since the volume of mSF was smaller than that of MSF, under the same mass fraction, there were more mSF; mSF filled the pores of the matrix, improving the matrix's compactness. It can also be seen that when the mSF content exceeded 0.3%, the increase in the compressive strength of the hybrid fiber group decreased: at this point, MSF dominated and had a greater impact on the compressive strength.
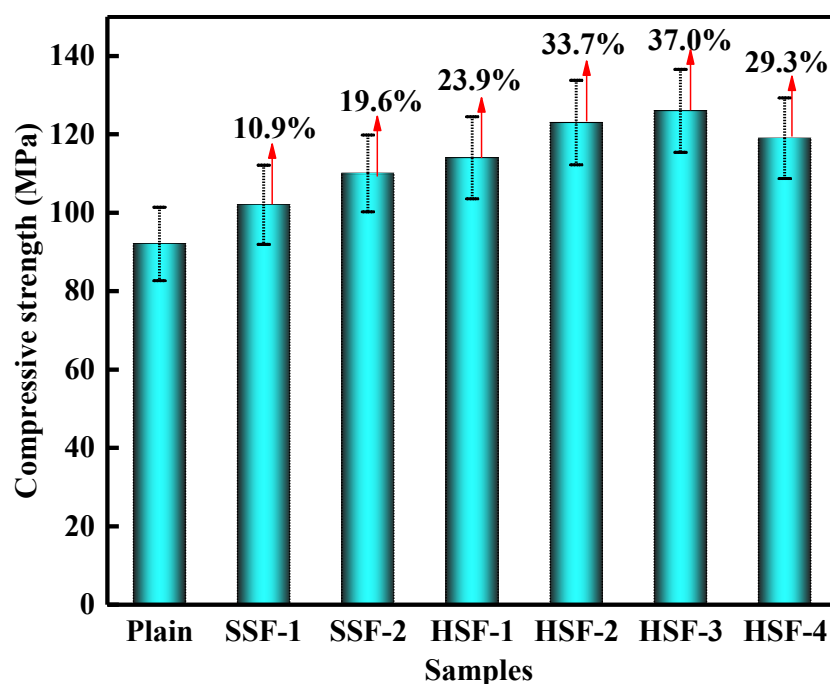

Figure 2. Compressive strength of FRC.

3.2. Flexural Strength

It can be seen from Figure 3 that the flexural strength and compressive strength have similar trends. Compared with the Plain group, the flexural strength of the FRC group was improved to varying degrees. The flexural strength of the SSF1 group increased by 10.7%, and the flexural strength of the SSF2 group increased by 42.2%. The enhancement effect of MSF content of 1.5% was better than that of MSF content in the 1.0% group. The flexural strength of the hybrid fiber group HSF1, HSF2, HSF3, and HSF4 increased by 51.4%, 84.9%, 88.1%, and 64.2%, respectively. It can be seen that the increase in the flexural strength of the HSF group was significantly greater than that of the Plain and SSF groups. ith the increase of mSF content, the increasing trend of flexural strength increases and decreases. When the mSF content is 0.3%, it reached the maximum. The synergistic effect of the hybrid fibers is greater than that of the single-doped MSF group: when the content of mSF exceeded 0.3%, the increase in flexural strength decreased. There are two main reasons for this. First, the small volume of mSF and the large content of mSF increased the amount of it in the matrix, which can easily lead to agglomeration in the body, thereby affecting the flexural strength of the matrix. Second, as the amount of MSF decreased, MSF's impact on the outcome became dominant. The amount of MSF significantly improves the matrix's crack resistance, such that the reduction of the amount of MSF reduces the flexural strength of the matrix.
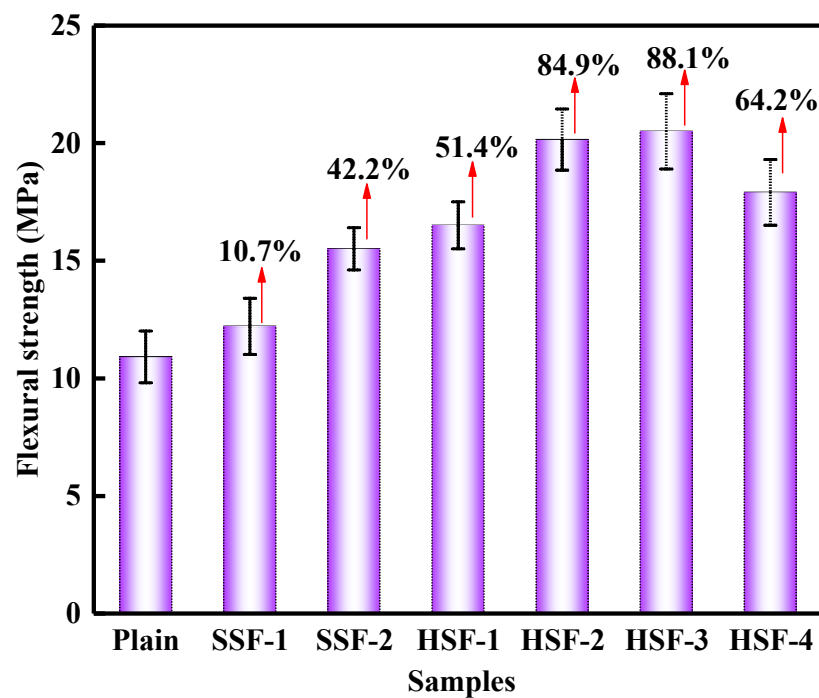
Figure 3. Flexural strength of FRC.

3.3. Flexural Strength to Compressive Strength Ratio

The ratio of flexural strength to compressive strength is important for measuring fiber-reinforced concrete's flexural strength. The flexural strength of concrete materials is usually positively correlated with compressive strength. The growth rate of the flexural strength is lower than the compressive strength. It can be seen from Figure 4 that the ratio of flexural strength to compressive strength of the Plain group is 0.118. After adding MSF, FRC's flexural strength to compressive strength ratio increases. The flexural strength to compressive strength ratio of SSF1 is 0.119, and that of SSF2 is 0.141. SSF1 and SSF2 groups increased by 0.08% and 19.5%, compared with the Plain group. Along with the increase of MSF content, the ratio of flexural strength to compressive strength increased, indicating that MSF's flexural strength enhancement effect on FRC was greater than the compressive strength effect. When msF was added, the ratios of flexural strength to compressive strength of HSF1, HSF2, HSF3, and HSF4 were 0.145, 0.164, 0.163, and 0.15, respectively. Compared with the SSF2 group, the ratio of flexural strength to compressive strength of HSF1, HSF2, HSF3, and HSF4 were increased by 2.8%, 17.0%, 15.6%, and 6.3%, respectively, indicating that the mixing of mSF and MSF on the flexural strength of FRC was significantly better than the SSF group. The hybrid fibers significantly improved the toughness of the FRC. In addition, it can be concluded that with the increase of mSF content, the specimen's flexural strength to compressive strength ratio increases first and then decreases. HSF2 (mSF is 0.2%, MSF is 1.3%) has the highest ratio of flexural strength to compressive strength; HSF4 (mSF is 0.5%, MSF is 1%), compared with the HSF2 group, is reduced by 8.5%, which indicates that when the mSF is less than 0.3%, the enhancement effect of mSF on the flexural strength is dominant in the HSF group. When mSF is greater than 0.3%, MSF's enhancement effect is greater than mSF, and MSF plays a dominant role in flexural strength. From the changing trend of the ratio of flexural strength to compressive strength, it can be concluded that the synergistic effect of the HSF group is significantly better than that of SSF, which significantly improves the toughness of FRC.
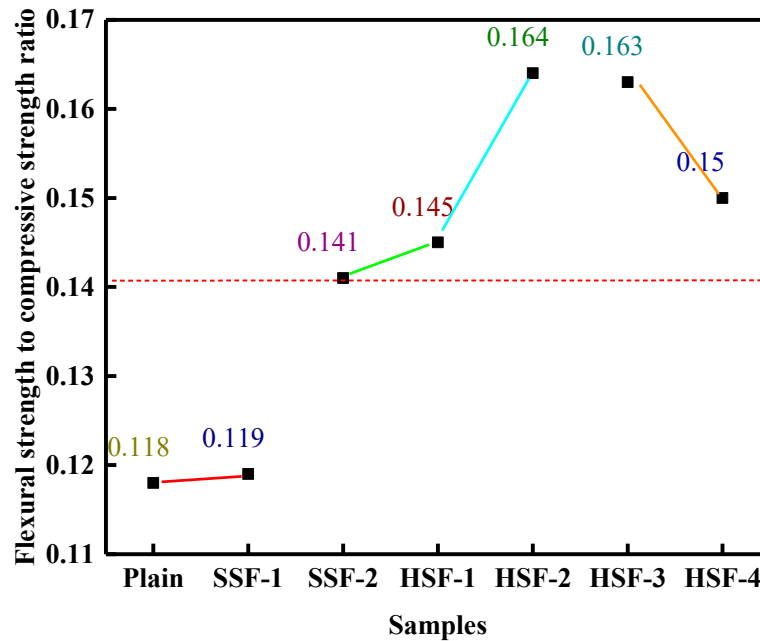
Figure 4. Ratio of flexural strength to compressive strength of FRC.

3.4. Toughness

The typical load–deflection curve of fiber-reinforced concrete is shown in Figure 5. It mainly includes three stages corresponding to the OA, AE, and EJ sections in Figure 5. The OA section is the elastic stage. When the sample is loaded, the load–deflection curve of the sample is a straight line. In the AE section, the load on the sample continues to increase until the first crack occurs. Point A is the initial crack point, and the AE section is the deflection-hardening stage. At this stage, the crack gradually increases and develops from a micro-crack to a macro-crack. The presence of fibers will play a role in preventing cracks, and the sample will exhibit multi-crack cracking. As the load increases, the crack expands to the main crack, and the fiber begins to be pulled out or broken from the matrix. At this time, it enters the third stage, the EJ section, which is the deflection-softening stage. As the load continues to increase, the cracks in the sample continue to extend until the cracks penetrate the entire sample, the sample is destroyed, and the test is ended.
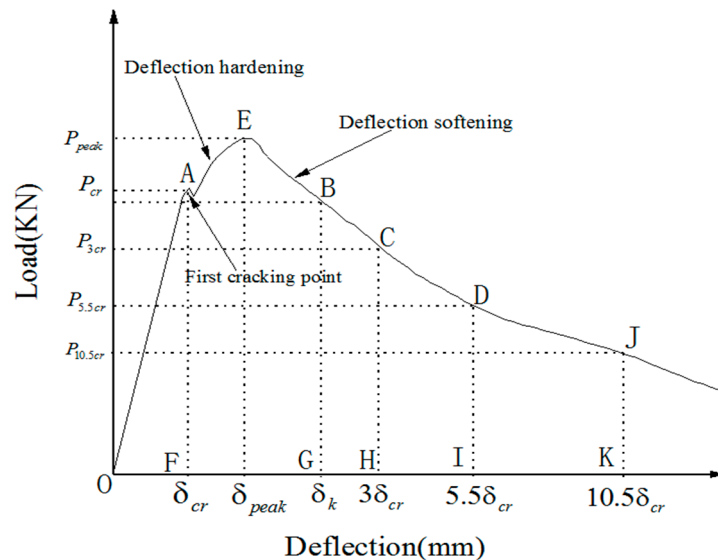

Figure 5. Typical load–deflection curve of FRC [32].

It can be seen from Figure 6 that after the load of the Plain group reached the peak value, the corresponding deflection reached the maximum value, and then the specimen failed suddenly, which is a brittle failure. After adding MSF, the load–deflection curve of the specimen is a full curve. As the load reached the peak, the specimen deflection continued to increase until the specimen was destroyed. It can be seen that after the specimen reaches the peak, the load–deflection curve appears smaller; floating fluctuations are caused by the continuous pulling or breaking of fibers. After adding fiber, the specimen changed from a brittle failure state to a ductile failure state; when the MSF content increased from 1% to 1.5%, the peak load, deflection, and load–deflection curve of the specimen all increased. After adding the hybrid fiber, compared with the Plain group and the SSF group, the peak load and deflection of the HSF group increased. It can be seen that with the increase of the mSF content, the peak load of the sample increased first and then decreased; when the content of mSF was 0.3% and the content of MSF was 1.2% in the HSF3 group, the peak load reached the maximum value; the peak load of the HSF4 group was reached with 0.5% mSF content and 1% MSF content, which was smaller than that of HSF2 and HSF3, and the residual deflection curve after the peak is also smaller of HSF2 and HSF3 groups. This is because the MSF content was 1%, compared with HSF1. In HSF2 and HSF3 group, the amount of MSF was lower, and the effect of MSF on fiber-cracking was dominant. When the load was applied to the specimen, the amount of MSF was lower, and the cracking resistance ability of the fiber was weakened. After the peak load was exceeded, the residual deflection decreased rapidly, and it can be seen that the curve is not smooth and has different degrees of fluctuation, which shows that the MSFs were constantly being pulled off or pulled out.
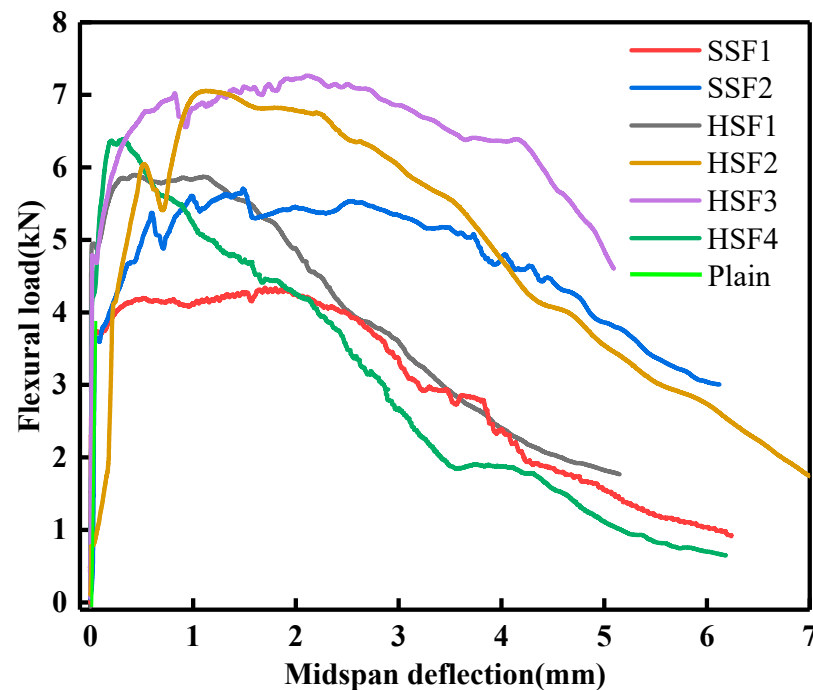

Figure 6. Load–deflection of FRC.

Flexural toughness was calculated according to the standard (Standard for Fiber Concrete Test Methods) CECS13-2009, which includes flexural toughness index and equivalent compressive strength.

$$f_{cr} = \frac{F_{cr}L}{bh^2} \tag{1}$$

where, f_{cr} is the initial crack strength, Mpa, F_{cr} is the initial load, N, L is the span, mm. The

toughness index of the specimen was calculated according to Formulas (2)–(4).

$$I_5 = \frac{\Omega_{3\delta}}{\Omega_\delta} \tag{2}$$

$$I_{10} = \frac{\Omega_{5.5\delta}}{\Omega_\delta} \tag{3}$$

$$I_{20} = \frac{\Omega_{10.5\delta}}{\Omega_\delta} \tag{4}$$

$$f_e = \frac{\Omega_k L}{bh^2 \delta_k} \tag{5}$$

$$R_e = \frac{f_e}{f_{cr}} \tag{6}$$

Figure 7 shows the initial crack strength of the specimen. It can be seen that after adding mSF, the initial crack strength of the HSF group is significantly greater than that of the SSF2 group, and the initial crack strengths of SSF1, SSF2, HSF1, HSF2, HSF3, HSF4 are 7.01 MPa, 6.86 MPa, 9.28 MPa, 7.74 MPa, 8.97 MPa, 7.87 MPa, respectively. Compared with the SSF2 group, the initial crack strengths of the HSF1, HSF2, HSF3, and HSF4 groups were increased by 35.3%, 12.8%, 30.8%, and 14.7%, respectively, indicating that the HSF groups have higher loads and deflections. It can be seen that the HSF4 group has the largest increase in initial crack strength, indicating that the HSF group exhibits a significant synergistic effect.
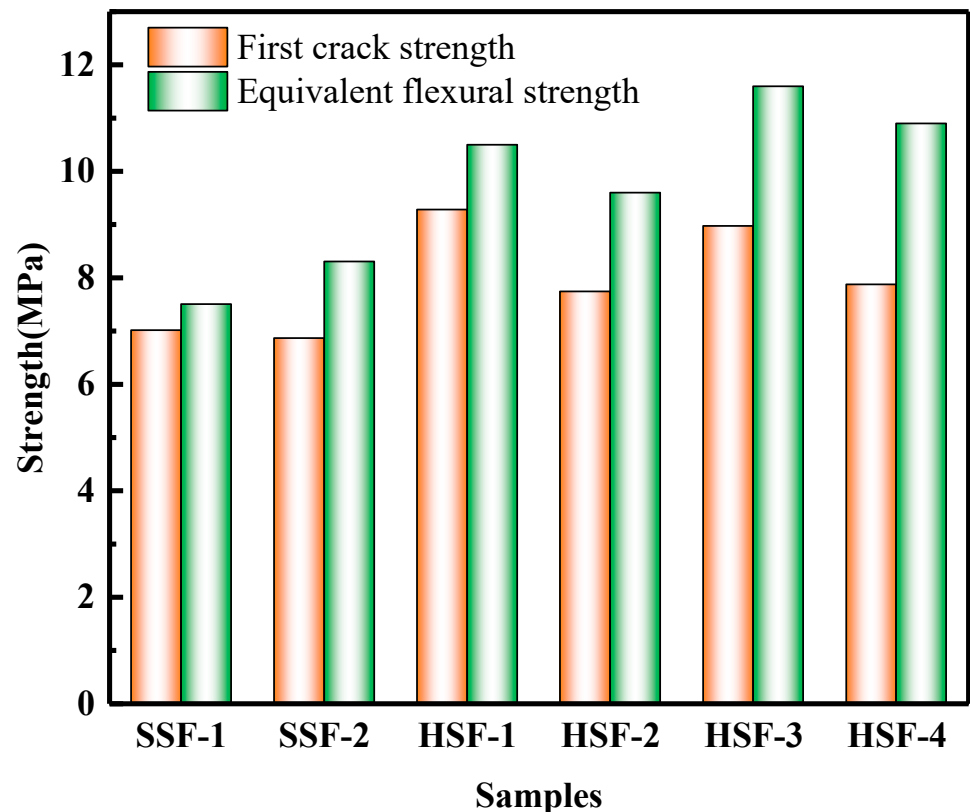

Figure 7. Different strengths of FRC.

Figure 8 shows the toughness index of the specimen. Due to the use of hybrid fibers, the toughness index of the HSF group is greater than that of the SSF1 and SSF2 groups. When the content of mSF is 0.2% and the content of MSF is 1.3%, I_5, I_{10}, and I_{20} reach the maximum value, which is 7.6, 17.87, and 39, respectively. It can be concluded that

mSF played an important role in improving the toughness of concrete within a reasonable content range.
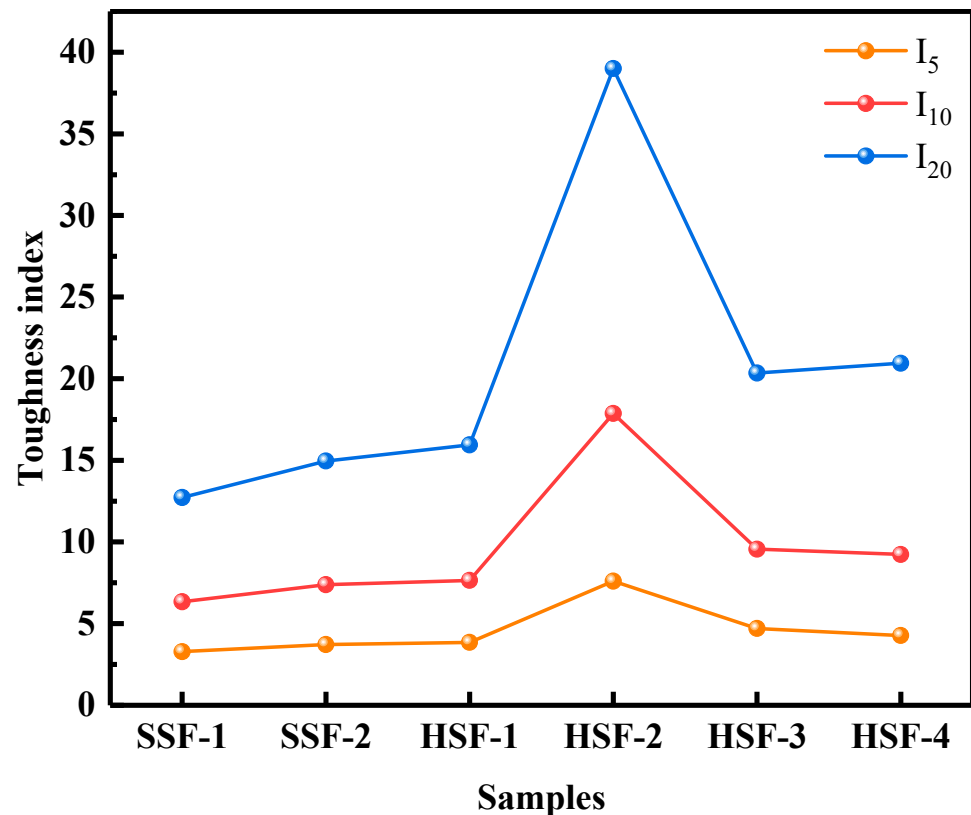

Figure 8. Toughness index of FRC.

The equivalent flexural strength of the specimen was calculated according to Equation (5) and the flexural toughness ratio of the specimen was calculated according to Equation (6). The equivalent flexural strength is shown in Figure 7. The equivalent flexural strengths of SSF1, SSF2, HSF1, HSF2, HSF3, HSF4 are 7.5 MPa, 8.3 MPa, 10.5 MPa, 9.6 MPa, 11.6 MPa, 10.9 MPa, respectively. After adding mSF fiber, the equivalent compressive strength of the HSF group was improved to different degrees. Compared with the SSF2 group, the equivalent compressive strengths of HSF1, HSF2, HSF3, and HSF4 increased by 26.5%, 15.7%, 39.8%, and 31.3%, respectively. It can be seen that when the mSF content is 0.3%, the MSF content is 1.2%. When the equivalent compressive strength of the HSF3 group reached the maximum value, the HSF group showed an obvious synergistic effect compared with the SSF group. The calculation results of the toughness ratio are shown in Figure 9. The toughness ratios of each group are 1.07, 1.21, 1.31, 1.24, 1.29, and 1.39, respectively. It can be seen that after adding mSF, the toughness ratio of the HSF group is improved to varying degrees. Compared with the SSF2 group, the toughness ratios of HSF1, HSF2, HSF3, and HSF4 were increased by 9.2%, 3.3%, 7.7%, and 15.4%, respectively, and the toughness ratio of the HSF4 group was the largest. Combining the changes in initial crack strength, equivalent flexural strength, toughness index, and toughness ratio, it can be concluded that the HSF group showed a significant synergistic effect, and the toughness and strength of the FRC were improved significantly more than those of the SSF group.
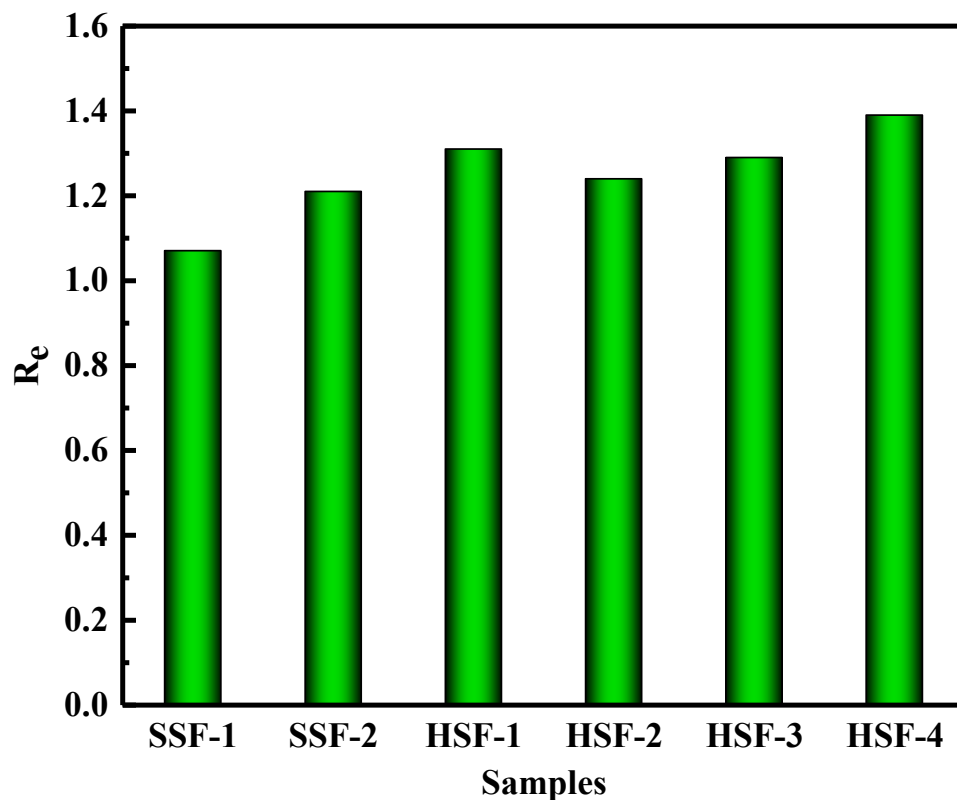
Figure 9. Toughness ratio of FRC.

3.5. Resistance to Sulfate Erosion

1.   Corrosion resistant coefficient:

$$K_s = \frac{f_s}{f_w} \tag{7}$$

where K_s is the corrosion resistant coefficient, f_s is the flexural strength after sulfate erosion, f_w is the flexural strength curing in water.

2.   Mass-loss rate:

$$W_s = \frac{m_b - m_s}{m_b} \tag{8}$$

where W_s is mass-loss rate, m_b is the mass of the sample before sulfate erosion, m_s is the mass of the sample after sulfate erosion.

The sulfate corrosion resistance coefficient of the specimen can be calculated according to Equation (7). As shown in Figure 10a, each specimen's sulfate corrosion resistance coefficient increases with the corrosion time, and the higher the corrosion coefficient, the higher the sulfate resistance., and the better the erosion performance. After 28 days, 56 days, 90 days, 120 days, 150 days, and 180 days of erosion, the erosion resistance coefficients of the Plain group were 1.01, 1.04, 1.07, 1.09, 1.11, 1.12, respectively, indicating that sulfoaluminate cement has excellent resistance to sulfuric acid salt erosion. The sulfate corrosion resistance coefficients of the SSF group and the HSF group at each erosion age were larger than those of the Plain group. Along with the increase of mSF content, the sulfate corrosion resistance coefficient of the HSF group at the same time increased first and then decreased. The sulfate corrosion resistance coefficient of the HSF3 group reached the maximum value of 1.08, 1.1, 1.16, 1.18, 1.19, and 1.22, respectively. Hybrid fibers within a suitable fiber content range are beneficial to improving the ability of sulfoaluminate cement to resist sulfate attack.
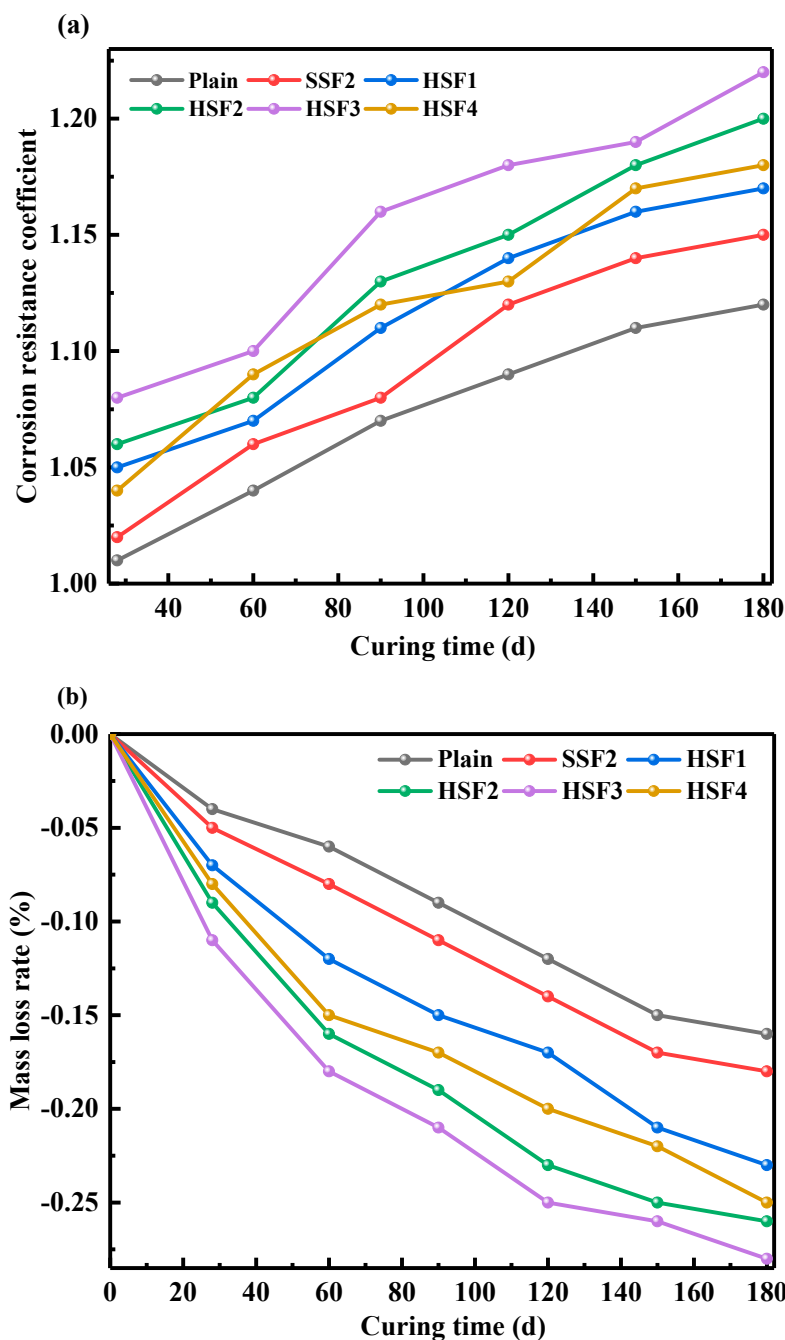
(a)

(b)

Figure 10. Corrosion resistance coefficient and mass loss rate of FRC.

Figure 10b shows the mass-loss rate of the specimen at different erosion ages, and the mass-loss rate is negative, indicating that the mass of the specimen increases after sulfate erosion. It can be seen that the mass of the specimens in each group shows an increasing trend with the increase of the erosion age. The mass-growth rates of the Plain group were 0.04, 0.06, 0.09, 0.12, 0.15, and 0.16, and after adding 1.5% MSF, the growth rates of SSF2 were 0.05, 0.08, 0.11, 0.14, 0.17, and 0.18, respectively. After adding mSF fibers, the mass-growth rate of the sample first increased and then decreased with the increase of the mSF content. When the mSF content was 0.3%, and the MSF content was 1.2%, the mass-growth rate of the sample HSF3 reached the maximum, 0.11, 0.18, 0.21, 0.25, 0.26, and 0.28, respectively. This shows that after sulfate corrosion, the specimen's interior is entered, and a chemical reaction occurs. The specimen generates AFt from the inside to the outside so that the mass will increase. In addition, in the long-term sulfate attack test, the

hydration of C_2S in sulfoaluminate cement will generate a small amount of CH (Calcium hydroxide) and sulfate ion, and CH and AH_3, which react to generate AFt, which further fills the pores and increases the compactness of the matrix. Therefore, the flexural strength of the matrix increases after a sulfate attack. However, with the extension of the erosion age, AFt is continuously generated, and the pores are filled. When the cement matrix itself cannot resist the expansion stress of AFt, the internal structure of the cement matrix will be destroyed. In addition, when the amount of gypsum is insufficient in SAC cement, the hydration reaction will generate AFm, and AFm will react with sulfate to generate AFt; the sulfate erosion resistance mechanism of hybrid fiber reinforced concrete is shown in Figures 11 and 12.
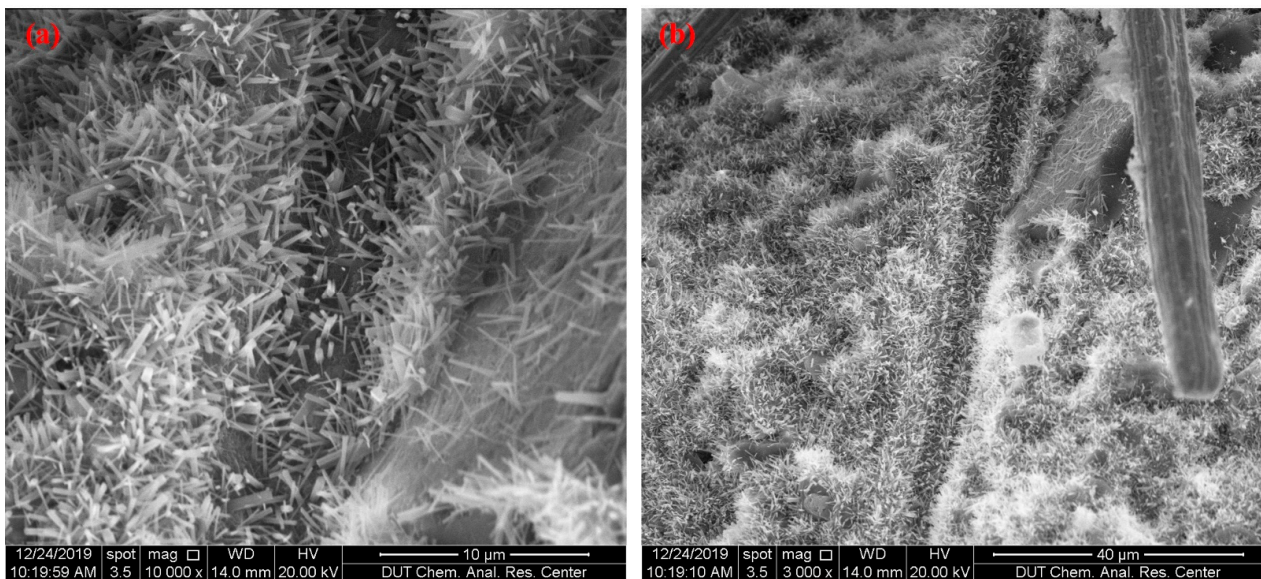

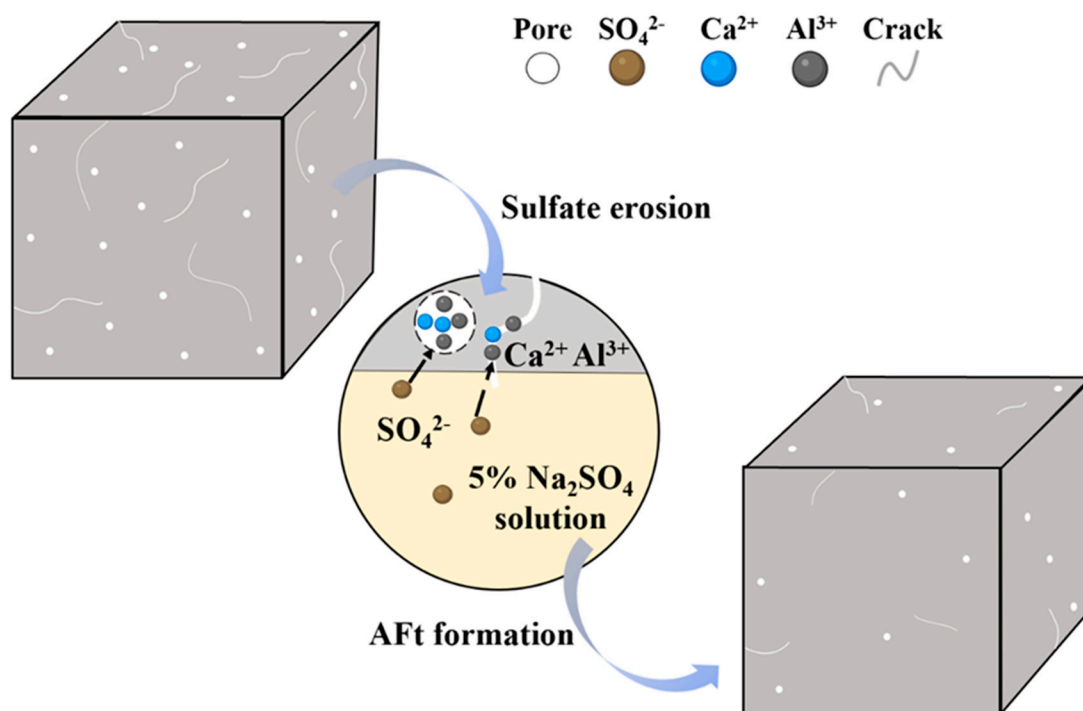**Figure 11.** Morphology of FRC after sulfate attack.

Figure 12. Mechanism diagram of FRC resistance to sulfate erosion.

Figure 13 shows the morphology of mSF in the matrix. When the load plays on the matrix, the mSF can transmit the stress and redistribute the stress in the matrix, and the crack development extends to the mSF. The mSF changes and delays the development path of the crack, dissipates the energy, and improves the flexural toughness of the matrix. It can be seen that after the mSF is pulled out, cracks appear in the pores, indicating that the matrix and the mSF are tightly connected. The mSF delays the development of cracks through filling, bridging, contortion, bonding, pull-off, and pull-out. When the crack develops into a macro-crack, MSF hinders the development of macro-cracks, forming a multi-scale crack-stopping mechanism for hybrid fibers. MSF bridges macro-cracks and mSF bridges micro-cracks, such that two different scales of steel fibers, through filling, bridging, anchoring, pulling off, and pulling out, improve the toughness of composite materials.
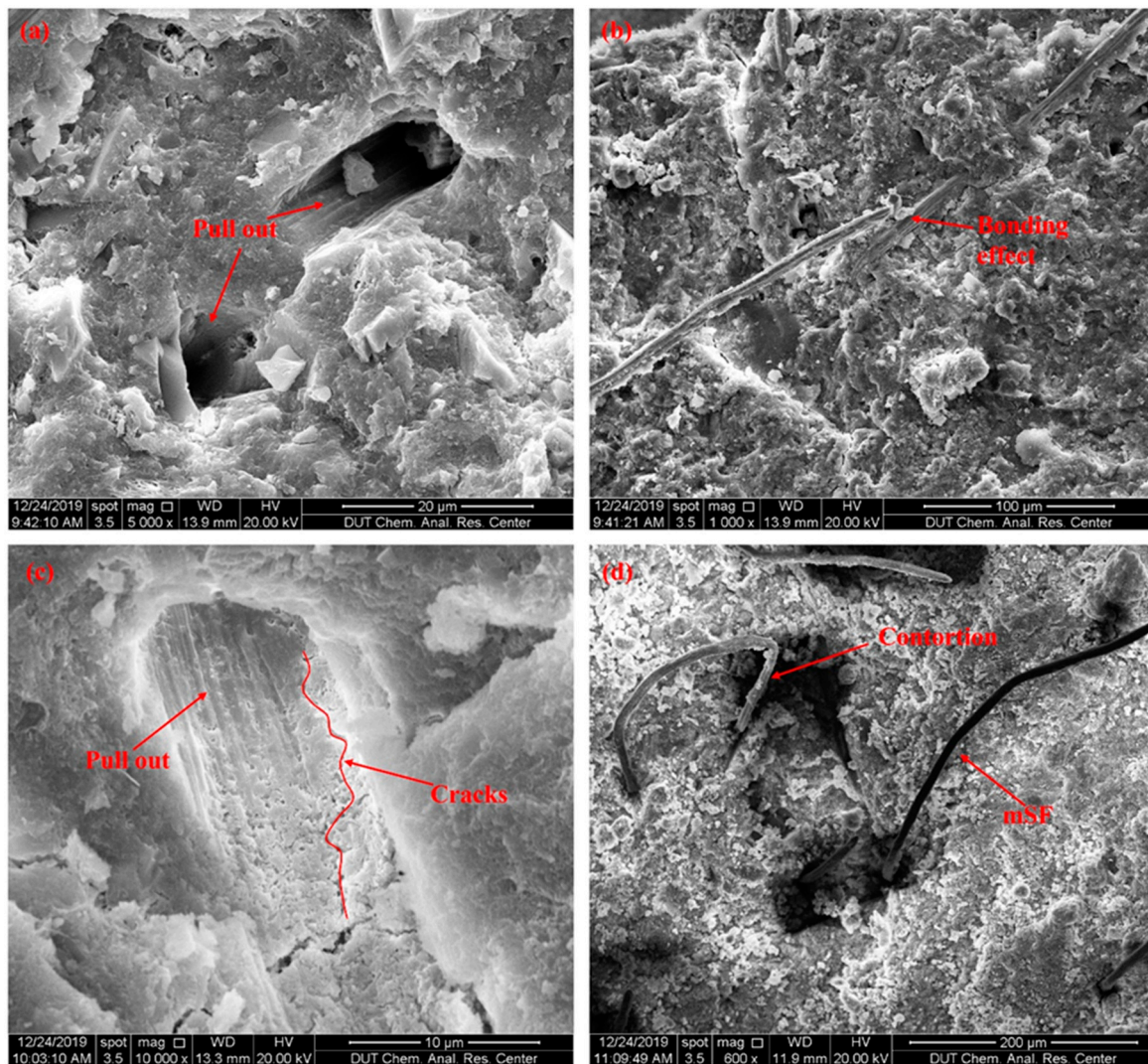

Figure 13. Morphology of mSF in FRC.

4. Conclusions

This paper developed a sulfoaluminate cement-based material with good durability and high toughness. The mechanical properties of different scales of steel-fiber-reinforced sulfoaluminate cement-based composites were mainly studied, including compressive strength, flexural strength, toughness index, and toughness ratio, and the resistance to sulfate erosion was characterized. The main conclusions are shown below.

1. Adding MSF and HSF can significantly improve concrete's compressive and flexural strength compared with the Plain group.
2. Compared with the Plain group, the compressive strength of SSF1 (1% MSF) and SSF2 (1.5% MSF) increased by 10.9%, 19.6%, and the compressive strength of HSF1 (0.1% mSF, 1.4% MSF), HSF2 (0.2% mSF, 1.3% MSF), HSF3 (0.3% mSF, 1.2% MSF), HSF4 (0.5% mSF, 1.0% MSF) increased by 23.9%, 33.7%, 37.0%, 29.3%, respectively.
3. Compared with the Plain group, the flexural strength of HSF1, HSF2, HSF3, HSF4 groups increased by 51.4%, 84.9%, 88.1%, and 64.2%.
4. Compared with the SSF group, the HSF group has higher initial crack strength and equivalent flexural strength, toughness index, and toughness ratio. Hybrid fibers have a higher synergistic effect.
5. The mechanism of multi-scale reinforcement of hybrid steel fibers enhances sulfoaluminate cement-based composites: mSF bridges micro-cracks, MSF bridges macro-cracks, and two different scales of steel fibers, through filling, bridging, anchoring, pulling off, and pulling out, improve the toughness of composite materials.
6. The mechanism of sulfate corrosion resistance of sulfoaluminate cement-based composites was obtained. SO_4^{2-} entered the matrix and reacted and formed AFt, filling the matrix's pores. The whole process is similar to the self-healing process of concrete.

References

1. Fu, C.; Ye, H.; Wang, K.; Zhu, K.; He, C. Evolution of mechanical properties of steel fiber-reinforced rubberized concrete (FR-RC). *Compos. Part B Eng.* **2019**, *160*, 158–166. [CrossRef]
2. Cui, K.; Liang, K.; Chang, J.; Lau, D. Investigation of the macro performance, mechanism, and durability of multiscale steel fiber reinforced low-carbon ecological UHPC. *Constr. Build. Mater.* **2022**, *327*, 126921. [CrossRef]
3. Bencardino, F.; Rizzuti, L.; Spadea, G.; Swamy, R.N. Experimental evaluation of fiber reinforced concrete fracture properties. *Compos. Part B Eng.* **2010**, *41*, 17–24. [CrossRef]
4. Lee, J. Influence of concrete strength combined with fiber content in the residual flexural strengths of fiber reinforced concrete. *Compos. Struct.* **2017**, *168*, 216–225. [CrossRef]
5. Sirijaroonchai, K.; El-Tawil, S.; Parra-Montesinos, G. Behavior of high performance fiber reinforced cement composites under multi-axial compressive loading. *Cem. Concr. Compos.* **2010**, *32*, 62–72. [CrossRef]
6. Kazemi, M.T.; Golsorkhtabar, H.; Beygi, M.H.A.; Gholamitabar, M. Fracture properties of steel fiber reinforced high strength concrete using work of fracture and size effect methods. *Constr. Build. Mater.* **2017**, *142*, 482–489. [CrossRef]
7. Cui, K.; Chang, J.; Feo, L.; Chow, C.L.; Lau, D. Developments and Applications of Carbon Nanotube Reinforced Cement-Based Composites as Functional Building Materials. *Front. Mater.* **2022**, *9*, 146. [CrossRef]
8. Cui, K.; Lau, D.; Zhang, Y.; Chang, J. Mechanical properties and mechanism of nano-$CaCO_3$ enhanced sulphoaluminate cement-based reactive powder concrete. *Constr. Build Mater.* **2021**, *309*, 125099. [CrossRef]
9. Du, Y.; Yang, J.; Skariah Thomas, B.; Li, L.; Li, H.; Mohamed Shaban, W.; Wai, T. Influence of hybrid graphene oxide/carbon nanotubes on the mechanical properties and microstructure of magnesium potassium phosphate cement paste. *Constr. Build. Mater.* **2020**, *260*, 120449. [CrossRef]
10. Mansouri Sarvandani, M.; Mahdikhani, M.; Aghabarati, H.; Haghparast Fatmehsari, M. Effect of functionalized multi-walled carbon nanotubes on mechanical properties and durability of cement mortars. *J. Build. Eng.* **2021**, *41*, 102407. [CrossRef]
11. Jung, M.; Lee, Y.; Hong, S.; Moon, J. Carbon nanotubes (CNTs) in ultra-high performance concrete (UHPC): Dispersion, mechanical properties, and electromagnetic interference (EMI) shielding effectiveness (SE). *Cem. Concr. Res.* **2020**, *131*, 106017. [CrossRef]

12. Cui, K.; Chang, J. Hydration, reinforcing mechanism, and macro performance of multi-layer graphene-modified cement composites. *J. Build. Eng.* **2022**, *57*, 104880. [CrossRef]

13. Cui, K.; Chang, J.; Sabri, M.M.S.; Huang, J. Influence of Graphene Nanoplates on Dispersion, Hydration Behavior of Sulfoaluminate Cement Composites. *Materials* **2022**, *15*, 5357. [CrossRef]

14. Cui, K.; Chang, J.; Sabri, M.M.S.; Huang, J. Study of Dispersion, Hydration, and Microstructure of Graphene Nanoplates-Modified Sulfoaluminate Cement Paste. *Nanomaterials* **2022**, *12*, 2708. [CrossRef]

15. Matalkah, F.; Soroushian, P. Graphene nanoplatelet for enhancement the mechanical properties and durability characteristics of alkali activated binder. *Constr. Build. Mater.* **2020**, *249*, 118773. [CrossRef]

16. Gong, P.; Zhang, C.; Wu, Z.; Zhang, G.; Mei, K.; Gao, Q.; Cheng, X. Study on the effect of $CaCO_3$ whiskers on carbonized self-healing cracks of cement paste: Application in CCUS cementing. *Constr. Build. Mater.* **2022**, *321*, 126368. [CrossRef]

17. Li, M.; Yang, Y.; Liu, M.; Guo, X.; Zhou, S. Hybrid effect of calcium carbonate whisker and carbon fiber on the mechanical properties and microstructure of oil well cement. *Constr. Build. Mater.* **2015**, *93*, 995–1002. [CrossRef]

18. Kim, G.M.; Yang, B.J.; Yoon, H.N.; Lee, H.K. Synergistic effects of carbon nanotubes and carbon fibers on heat generation and electrical characteristics of cementitious composites. *Carbon* **2018**, *134*, 283–292. [CrossRef]

19. Stynoski, P.; Mondal, P.; Marsh, C. Effects of silica additives on fracture properties of carbon nanotube and carbon fiber reinforced Portland cement mortar. *Cem. Concr. Compos.* **2015**, *55*, 232–240. [CrossRef]

20. Zhou, A.; Qiu, Q.; Chow, C.L.; Lau, D. Interfacial performance of aramid, basalt and carbon fiber reinforced polymer bonded concrete exposed to high temperature. *Compos. Part A Appl. Sci. Manuf.* **2020**, *131*, 105802. [CrossRef]

21. Wu, Z.; Shi, C.; He, W.; Wu, L. Effects of steel fiber content and shape on mechanical properties of ultra high performance concrete. *Constr. Build. Mater.* **2016**, *103*, 8–14. [CrossRef]

22. Abbass, W.; Khan, M.I.; Mourad, S. Evaluation of mechanical properties of steel fiber reinforced concrete with different strengths of concrete. *Constr. Build. Mater.* **2018**, *168*, 556–569. [CrossRef]

23. Mohod, A.V.; Gogate, P.R. Ultrasonic degradation of polymers: Effect of operating parameters and intensification using additives for carboxymethyl cellulose (CMC) and polyvinyl alcohol (PVA). *Ultrason. Sonochem.* **2011**, *18*, 727–734. [CrossRef]

24. Wang, D.; Ju, Y.; Shen, H.; Xu, L. Mechanical properties of high performance concrete reinforced with basalt fiber and polypropylene fiber. *Constr. Build. Mater.* **2019**, *197*, 464–473. [CrossRef]

25. Qin, J.; Qian, J.; Li, Z.; You, C.; Dai, X.; Yue, Y.; Fan, Y. Mechanical properties of basalt fiber reinforced magnesium phosphate cement composites. *Constr. Build. Mater.* **2018**, *188*, 946–955. [CrossRef]

26. Yu, S.; Bale, H.; Park, S.; Hwang, J.Y.; Hong, S.H. Anisotropic microstructure dependent mechanical behavior of 3D-printed basalt fiber-reinforced thermoplastic composites. *Compos. Part B Eng.* **2021**, *224*, 109184. [CrossRef]

27. Li, B.; Chi, Y.; Xu, L.; Shi, Y.; Li, C. Experimental investigation on the flexural behavior of steel-polypropylene hybrid fiber reinforced concrete. *Constr. Build. Mater.* **2018**, *191*, 80–94. [CrossRef]

28. Huang, L.; Xu, L.; Chi, Y.; Xu, H. Experimental investigation on the seismic performance of steel–polypropylene hybrid fiber reinforced concrete columns. *Constr. Build. Mater.* **2015**, *87*, 16–27. [CrossRef]

29. Banthia, N.; Majdzadeh, F.; Wu, J.; Bindiganavile, V. Fiber synergy in Hybrid Fiber Reinforced Concrete (HyFRC) in flexure and direct shear. *Cem. Concr. Compos.* **2014**, *48*, 91–97. [CrossRef]

30. Wu, Z.; Khayat, K.H.; Shi, C. How do fiber shape and matrix composition affect fiber pullout behavior and flexural properties of UHPC? *Cem. Concr. Compos.* **2018**, *90*, 193–201. [CrossRef]

31. Gao, D.; Zhang, L. Flexural performance and evaluation method of steel fiber reinforced recycled coarse aggregate concrete. *Constr. Build. Mater.* **2018**, *159*, 126–136. [CrossRef]

32. Chang, J.; Cui, K.; Zhang, Y. Effect of hybrid steel fibers on the mechanical performances and microstructure of sulphoaluminate cement-based reactive powder concrete. *Constr. Build. Mater.* **2020**, *261*, 120502. [CrossRef]